Comparative Metabolomics Reveals Biogenesis of Ascarosides, a Modular Library of Small-Molecule Signals in *C. elegans*

Stephan H. von Reuss,[†] Neelanjan Bose,[†] Jagan Srinivasan,[‡] Joshua J. Yim,[†] Joshua C. Judkins,[†] Paul W. Sternberg,[‡] and Frank C. Schroeder*[,†]

[†]Boyce Thompson Institute and Department of Chemistry and Chemical Biology, Cornell University, Ithaca, New York 14853, United States

[‡]Howard Hughes Medical Institute and Division of Biology, California Institute of Technology, Pasadena, California 91125, United States

S *Supporting Information*

ABSTRACT: In the model organism *Caenorhabditis elegans*, a family of endogenous small molecules, the ascarosides function as key regulators of developmental timing and behavior that act upstream of conserved signaling pathways. The ascarosides are based on the dideoxysugar ascarylose, which is linked to fatty-acid-like side chains of varying lengths derived from peroxisomal β-oxidation. Despite the importance of ascarosides for many aspects of *C. elegans* biology, knowledge of their structures, biosynthesis, and homeostasis remains incomplete. We used an MS/MS-based screen to profile ascarosides in *C. elegans* wild-type and mutant metabolomes, which revealed a much greater structural diversity of ascaroside derivatives than previously reported. Comparison of the metabolomes from wild-type and a series of peroxisomal β-oxidation mutants showed that the enoyl CoA-hydratase MAOC-1 serves an important role in ascaroside biosynthesis and clarified the functions of two other enzymes, ACOX-1 and DHS-28. We show that, following peroxisomal β-oxidation, the ascarosides are selectively derivatized with moieties of varied biogenetic origin and that such modifications can dramatically affect biological activity, producing signaling molecules active at low femtomolar concentrations. Based on these results, the ascarosides appear as a modular library of small-molecule signals, integrating building blocks from three major metabolic pathways: carbohydrate metabolism, peroxisomal β-oxidation of fatty acids, and amino acid catabolism. Our screen further demonstrates that ascaroside biosynthesis is directly affected by nutritional status and that excretion of the final products is highly selective.
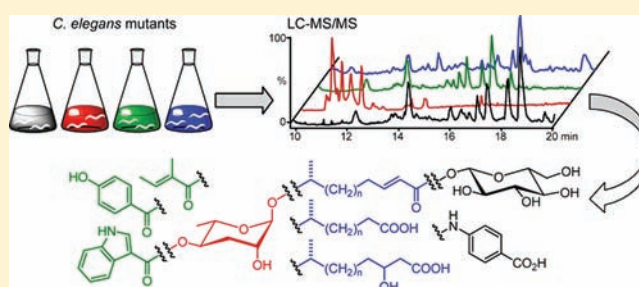
1. INTRODUCTION

Several different aspects of the life history of the nematode *Caenorhabditis elegans* are regulated by ascarosides, glycosides of the dideoxysugar ascarylose (Figure 1).[1−5] The ascarosides ascr#1−3 were originally identified as major components of the dauer pheromone, a population-density signal that promotes entry into an alternate larval stage, the nonfeeding and highly persistent dauer diapause.[1,2,4−6] Entry into the dauer stage is mediated by several highly conserved signaling pathways, including insulin/IGF-1 signaling and transforming growth factor beta (TGF-β) signaling,[7] which contributed to interest in the ascarosides' structures, their biosynthesis, and their mode of action. More recent work showed that specific mixtures of ascarosides including the 4-aminobenzoic acid derivative ascr#8 act as strong male-specific attractants,[3,5] whereas ascarosides including a tryptophan-derived indole-3-carboxy moiety function as aggregation signals at femtomolar concentrations.[8]

The biosynthetic pathways that control specific assembly of the ascarylose, lipid side chain, and peripheral building blocks are largely unknown. Earlier work showed that worms carrying a mutation in the gene *daf-22* are defective in the biosynthesis

of both the dauer pheromone and male-attracting signals.[3,9,10] *daf-22* encodes a protein with strong homology to human sterol carrier protein SCPx and in *C. elegans* functions in peroxisomal β-oxidation of long-chain fatty acids, producing the 3−9-carbon side chains of the ascarosides.[6] Two other components of peroxisomal β-oxidation were shown to participate in ascaroside biosynthesis: the acyl-CoA oxidase ACOX-1[11] and the β-hydroxyacyl-CoA dehydrogenase DHS-28,[6,12] a partial homologue of human multifunctional enzyme type 2 (MFE-2). However, the exact roles of these enzymes in ascaroside biosynthesis remained unclear, because the effects of *acox-1* and *dhs-28* mutations on ascaroside production were only partially characterized.

The recent discovery of new structural variants with important divergent functions, e.g., icas#3 and icas#9,[8,13] suggested that knowledge of ascaroside structures and functions in *C. elegans* remains incomplete. Results from biological studies further indicate that even small structural differences between
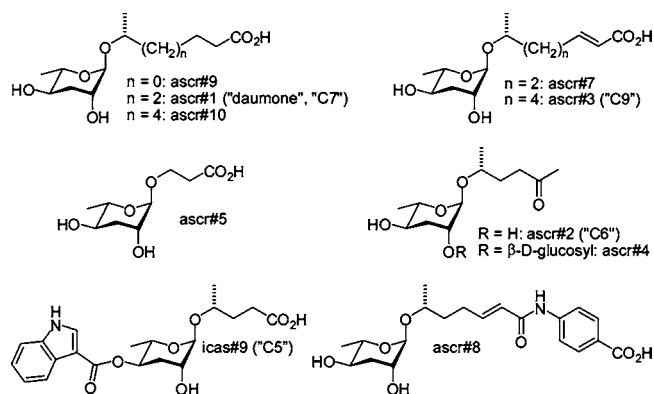
Figure 1. Ascarosides that regulate development and behavior in *C. elegans*: ascr#1−4, ascr#5, and icas#9 were identified via activity-guided fractionation;[1−4,13] ascr#7 and ascr#8 were identified using differential analysis of 2D NMR spectra;[5] and ascr#9 and #10 were detected using mass spectrometric techniques.[8]

ascarosides can be associated with significant functional differences; for example, ascr#3 is a potent male attractant, whereas the structurally similar ascr#7 is nearly inactive in this assay.[5,14] Correspondingly, several previous studies indicate that ascaroside biosynthesis is tightly controlled by environmental factors such as temperature, nutrient availability, and population density.[6,11,15] Therefore, detailed investigation of ascaroside structures and their biosynthetic pathways is essential for many aspects of the biology of this model organism.

In this study, we introduce HPLC-MS/MS-based metabolomics as a tool for ascaroside profiling in *C. elegans*. Application of this method to wild-type *C. elegans* revealed that the previously described ascarosides are part of a much larger, structurally diverse library of compounds derived from modular combination of building blocks from three different metabolic pathways. Subsequently we used HPLC-MS/MS of mutant metabolomes to interrogate ascaroside biosynthesis and homeostasis.

2. RESULTS

2.1. LC-MS/MS Reveals New Ascarosides in Wild-Type *C. elegans*. We aimed at developing a method that would (1) facilitate sensitive detection and quantitation of the known ascarosides in the metabolomes of different *C. elegans* strains and mutants and (2) aid with the discovery of new ascaroside derivatives. Because of the vast complexity of the *C. elegans* metabolome, HPLC-MS analysis of metabolite extracts results in extremely crowded chromatograms that are difficult to interpret (Figure 2a). However, it seemed likely that structurally related ascarosides would exhibit characteristic MS/MS fragmentation patterns, providing a much more selective and sensitive means for their detection. Therefore we investigated ESI MS/MS fragmentation of a series of synthetic ascarosides. We found that with negative-ion electrospray ionization (ESI⁻), ascarosides give rise to an intense and highly diagnostic product ion at m/z 73.02939 $[C_3H_5O_2]$ which originates from the ascarylose unit (Figures 2b and S1). This detection method proved suitable for all known ascarosides, except for ascr#2 and ascr#4 which do not ionize well under ESI⁻ conditions. For detection of ascarosides that ionize only under ESI⁺ conditions, we monitored neutral loss of 130.0663 amu $[C_6H_{10}O_3]$ due to cleavage of the ascarylose
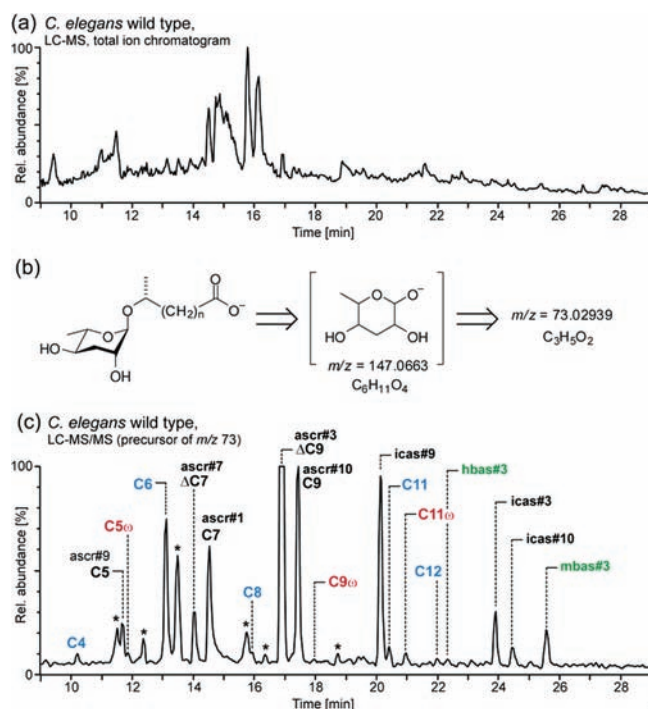

Figure 2. (a) LC-MS total ion current chromatogram of wild-type *C. elegans* excretome (ESI⁻). (b) MS/MS fragmentation of ascarosides. (c) LC-MS/MS screen (precursors of m/z 73) of wild-type excretome reveals known ascarosides (black), new homologues (blue), new ω-oxygenated isomers (red), and new 4′-acylated derivatives (green) (* indicates signals from non-ascarosides). The highly polar ascr#5 elutes at 6.5 min, outside of the retention time range shown.

unit; however, we found that ESI⁺ MS/MS detection of ascarosides is generally less sensitive than ESI⁻ MS/MS detection, as ascarosides fragment less predictably under ESI⁺ conditions. Next, we tested whether a screen for precursor ions of m/z 73 could be used to detect known as well as yet-unidentified ascarosides in the *C. elegans* wild-type metabolome. For this purpose we used liquid culture metabolite extracts, which contain accumulated excreted metabolites from large numbers of worms (the worm "excretome"). The resulting HPLC-MS/MS chromatograms showed a large number of well-resolved peaks, most of which we found to represent ascarosides, including several families of previously undetected compounds.

We first confirmed the identities of the known ascarosides using synthetic standards. In addition we found that the known saturated ascarosides ascr#1, ascr#9, and ascr#10 are accompanied by substantial quantities of homologues with 6−16-carbon side chains (Figures 2c and 3a). Identification of this homologous series was based on high-resolution MS/MS, LC retention times, and synthesis of representative members (see Supporting Information section 1.7 and Figure S2). The LC-MS/MS screen further revealed that ascarosides with side chains of 5−11 carbons are accompanied by smaller quantities of slightly less polar isomers. These ascaroside isomers are produced more abundantly by *acox-1* mutant worms (*vide infra*).

Several additional peaks in the wild-type MS/MS chromatograms could not be assigned to any of the known ascaroside classes. For two of these compounds, MS/MS product ions at m/z 301.1651 $[C_{15}H_{25}O_6]$ suggested that they represent ascr#3 derivatives. The putative ascr#3 derivatives were isolated by
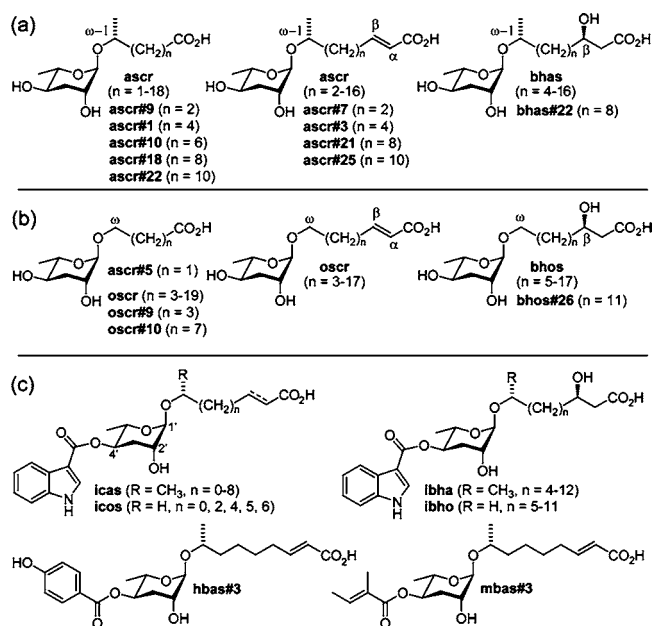
Figure 3. Ascarosides identified in wild-type, *acox-1*, *maoc-1*, *dhs-28*, and *daf-22* worms via LC-MS/MS: (a) (ω−1)-oxygenated ascarosides, (b) ω-oxygenated ascarosides, and (c) examples for 4′-acylated derivatives. The stereochemistry of compounds that were not synthesized (see Supporting Information for syntheses and a complete list of the 146 characterized ascarosides) was proposed as shown on the basis of analogy and HPLC-MS retention times (Figure S2).

preparative HPLC and analyzed using 2D NMR spectroscopy (dqfCOSY, see Figures S3 and S4), which confirmed that these compounds are ascr#3-based and further indicated the presence of a 4-hydroxybenzoyl or (*E*)-2-methyl-2-butenoyl (tigloyl) moiety attached to the 4-position of the ascarylose (Figure 3c). We corroborated these structural assignments via total synthesis of authentic samples (see Supporting Information). In analogy to the recently reported indole-3-carboxy derivative of ascr#3 ("icas#3"),[8] we named the 4-hydroxybenzoyl and (*E*)-2-methyl-2-butenoyl derivatives of ascr#3 with the small-molecule identifiers (SMIDs)[16] "hbas#3" and "mbas#3", respectively. hbas#3 and mbas#3 are the first ascarosides to incorporate 4-hydroxybenzoyl and (*E*)-2-methyl-2-butenoyl moieties, which in analogy to the indole-3-carboxy moiety in icas#3[8] could be derived from amino acid precursors. Because of structural similarity to the aggregation-inducing indole ascarosides,[8] we tested hbas#3 for its effect on worm behavior. We found that hbas#3 strongly attracts *C. elegans* at concentrations as low as 10 fM (see Figure S5), which exceeds the potency of any previously known *C. elegans* small-molecule signal.[3,8] Low femtomolar activity is unusual for small-molecule signals in animals but matched by some classes of peptide hormones.[17]

2.2. Peroxisomal β-Oxidation in Ascaroside Biosynthesis. Next we used comparative LC-MS/MS to investigate ascaroside biogenesis. Previous studies suggested that the side chains of the ascarosides are derived from peroxisomal β-oxidation of longer-chained precursors and that the acyl-CoA oxidase ACOX-1 participates in the first step of ascaroside side-chain β-oxidation, introducing α,β-unsaturation (Figure 4a,b).[11] In vertebrates as well as in *Drosophila*, the next two steps in peroxisomal β-oxidation, hydration of the double bond and subsequent dehydrogenation to the β-ketoacyl-CoA ester, are catalyzed by one protein, e.g., MFE-2. These two enzymatic

functions appear to be separated in *C. elegans* such that the hydratase and dehydrogenase are distinct proteins (Figure S6).[18] Previous work showed that *C. elegans* DHS-28, a protein with homology to the (*R*)-selective β-hydroxyacyl-CoA dehydrogenase domain of human MFE-2, likely participates in converting β-hydroxyacyl-CoA-derivatives into the corresponding β-ketoacyl-CoA intermediates, which are subsequently cleaved by the β-ketoacyl-CoA thiolase DAF-22.[6,12] However, it remained unclear which enzyme serves as the enoyl-CoA hydratase that catalyzes the essential second step of the β-oxidation cascade. Using our MS/MS-based ascaroside screen, we reinvestigated the ascaroside profiles of *acox-1*(*ok2257*), *dhs-28*(*hj8*), and *daf-22*(*ok693*) mutant worms. Additionally, we analyzed the excretomes of several other peroxisomal mutants, including *maoc-1*(*hj13*) worms, because a recent study indicated that *maoc-1* encodes a peroxisomal 2-enoyl-CoA hydratase,[19] which we hypothesized could participate in the hydration step of ascaroside β-oxidation.

2.3. Side-Chain Functionalization Precedes β-Oxidation. LC-MS/MS analysis of the excretome of *acox-1*(*ok2257*) mutant worms revealed that the abundance of the α,β-unsaturated ascr#3, the dominating component of wild-type media, was greatly reduced (Figure 4c). This decrease in ascr#3 and other α,β-unsaturated ascarosides does not appear to be the result of overall down-regulation in ascaroside production, but instead is accompanied by accumulation of a series of saturated ascarosides. For example, ascr#10, the dihydro derivative and direct precursor of ascr#3, is 13.6 times more abundant in *acox-1*(*ok2257*) than in the wild-type excretome. The corresponding homologues with 11- and 13-carbon side chains, ascr#18 and ascr#22, are 29 times and 66 times more abundant in *acox-1* than in the wild-type excretome, respectively. The buildup of longer chained saturated ascarosides in the *acox-1*(*ok2257*) excretome confirms the importance of ACOX-1 in α,β-dehydrogenation of the ascaroside side chain (Figure 4a). Because ascaroside biosynthesis is not abolished in *acox-1*(*ok2257*) worms, it seems likely that other, yet-unidentified ACOX-enzymes contribute to peroxisomal β-oxidation of long-chain ascaroside precursors. However, LC-MS/MS analysis of excretome of several other peroxisomal *acox* mutants (see Supporting Information, Figure S7) revealed largely wild-type-like ascaroside profiles.

Further analysis of the *acox-1*(*ok2257*) excretome revealed the complete absence of ascr#5, one of the major dauer-inducing ascarosides produced abundantly in wild-type (Figure 4d). Ascr#5 differs from all other previously identified ascarosides in that its side chain is attached to the ascarylose sugar via the terminal carbon ("ω linkage") and not the penultimate carbon ("ω−1 linkage") (Figure 3b). Instead of ascr#5, we detected large quantities of a new homologous series of saturated ascarosides in *acox-1*(*ok2257*), smaller amounts of which were also present in the wild-type excretome (Figure 4d). The most abundant component of this series of isomers was isolated via preparative HPLC and identified by NMR spectroscopy as an ω-linked ascaroside with a C_5 side chain (Figures 3b and S9). This suggested that the additional series of compounds observed in *acox-1* represents ω-linked saturated ascarosides (Table S2), which we confirmed by synthesis of C_5 and C_9 ω-linked ascarosides (see Supporting Information). In order to differentiate the ω-linked ascarosides from their previously described (ω−1)-linked isomers, we name the newly found ω-linked compounds with the SMID "oscr", e.g., the
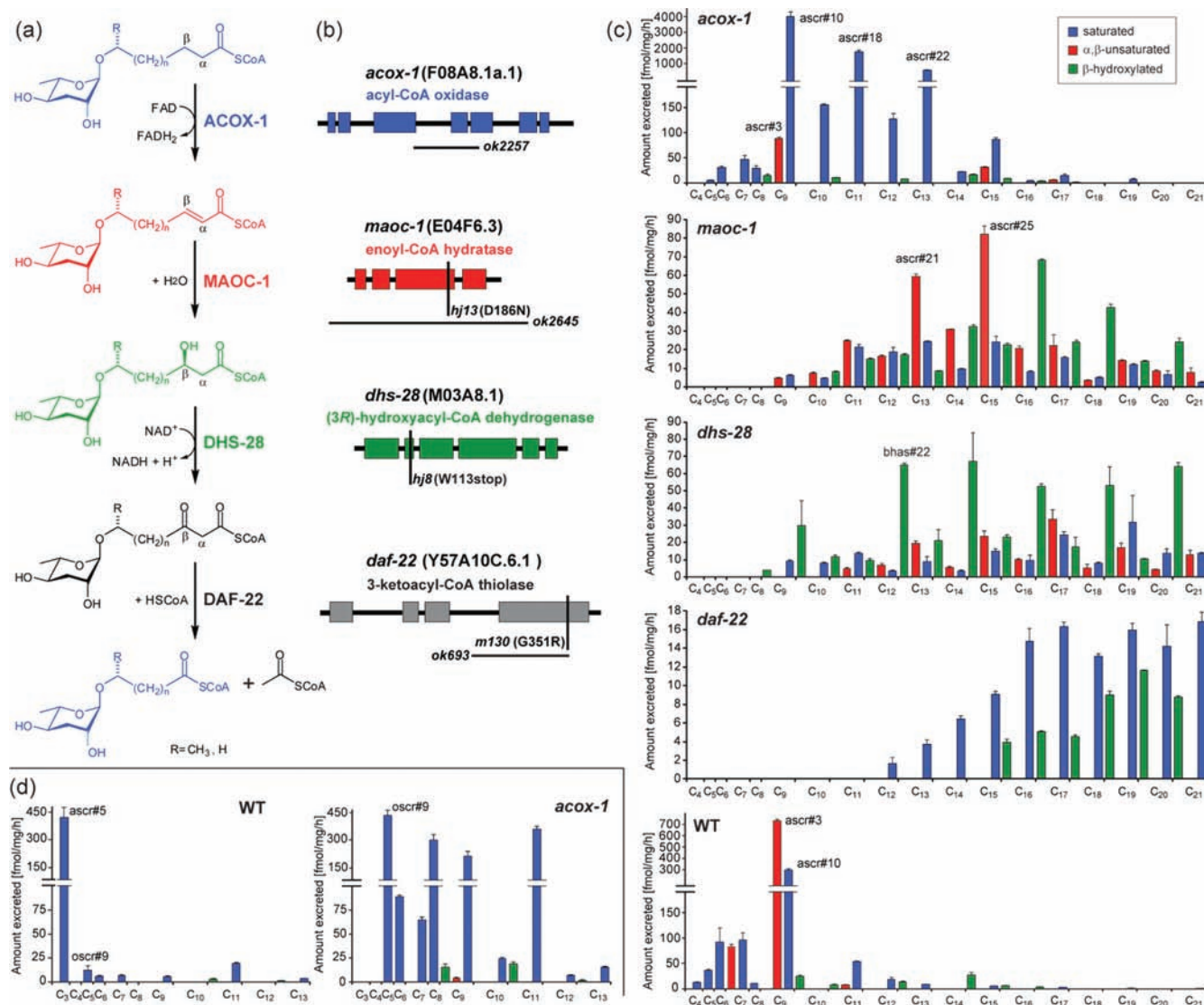
Figure 4. (a) Proposed roles of peroxisomal β-oxidation enzymes ACOX-1, MAOC-1, DHS-28, and DAF-22 in ascaroside biosynthesis. (b) Gene structures of *acox-1*, *maoc-1*, *dhs-28*, and *daf-22* mutant alleles, showing point mutations (vertical bars) and deletions (horizontal bars). (c) (ω−1)-Oxygenated ascarosides in wild-type and β-oxidation mutants (*acox-1*, *maoc-1*, *dhs-28*, and *daf-22*) with saturated (blue), α,β-unsaturated (red), and β-hydroxylated (green) side chains. (d) ω-Oxygenated ascarosides in wild-type and *acox-1* mutants (see also Figure S8).

synthesized ω-linked isomers of ascr#9 and ascr#10 were named oscr#9 and oscr#10 (Figure 3).

Thus production of ω-linked ascr#5 is abolished in *acox-1(ok2257)* worms, whereas production of longer chain homologues with 5−13-carbon side chains, e.g., oscr#9, is starkly upregulated (Figure 4d). These results indicate that β-oxidation in *acox-1(ok2257)* worms is strongly dependent on whether the side chain is (ω−1)- or ω-functionalized. Chain shortening of (ω−1)-oxygenated substrates appears to stall at a chain length of 9 carbons as in ascr#10, whereas ω-oxygenated substrates are processed for two additional rounds of β-oxidation to afford large quantities of ω-oxygenated oscr#9 featuring a 5-carbon side chain. This suggests that side-chain oxygenation precedes peroxisomal β-oxidation. In contrast, the time point of ascarylose attachment seems less certain. The absence of any (ω−1)- or ω-hydroxylated fatty acids in the investigated *C. elegans* mutant metabolome samples suggests a biosynthetic model in which very long-chain ascarosides (VLCAs) serve as substrates for peroxisomal β-oxidation;

however, the possibility that β-oxidation occurs prior to ascarylose attachment cannot be excluded.

2.4. MAOC-1 and DHS-28 Are Functional Homologues of Human MFE-2. In contrast to wild-type and *acox-1(ok2257)* worms, short-chain (<C_9) ascarosides were not detected in *maoc-1(hj13)* and *dhs-28(hj8)* worms, which instead accumulate several series of (ω−1)- and ω-oxygenated medium- and long-chain ascarosides (≥C_9). The ascaroside profile of the *maoc-1(hj13)* excretome was dominated by α,β-unsaturated ascarosides such as ascr#21 (C_{13}) and ascr#25 (C_{15}) (Figure 4c), supporting our hypothesis that MAOC-1 functions as an enoyl-CoA hydratase in the ascaroside biosynthetic pathway (Figure 4a). In addition, the *maoc-1(hj13)* excretome contained smaller amounts of the corresponding saturated ascarosides, along with a third homologous series of compounds, whose HRMS and MS/MS fragmentation suggested that they represent a series of long-chain β-hydroxylated ascarosides (Figures 4c and S1, Tables S3 and S4). These structural assignments were confirmed via synthesis of representative members of this series (see

Supporting Information), the C_9 and C_{13} β-hydroxylated (ω−1)-ascarosides, bhas#10 and bhas#22, as well as the C_{15} β-hydroxylated ω-ascaroside bhos#26 [SMIDs for (ω−1)- and ω-oxygenated β-hydroxylated ascarosides are bhas and bhos]. Since β-hydroxylated ascarosides are putative products of enoyl-CoA hydratases such as MAOC-1, their presence in the excretomes of both studied *maoc-1* mutant strains, *maoc-1(hj13)*, which carries a point mutation in the active site (D186N), and the 2110 base pair deletion mutant *maoc-1(ok2645)* (Figure 4b), suggests that additional enoyl-CoA hydratases may participate in ascaroside biosynthesis.

Similar to our results for *maoc-1(hj13)*, we found that the *dhs-28(hj8)* ascaroside profile is dominated by compounds with side chains ranging from C_9–C_{21} (Figure 4c). However, in contrast to *maoc-1(hj13)*, saturated and α,β-unsaturated ascarosides constitute a relatively smaller portion of total ascarosides in *dhs-28(hj8)*. Instead, we found (ω−1)- and ω-oxygenated β-hydroxyascarosides (bhas and bhos) with odd-numbered side chains from C_{13}–C_{21} as major components (Figures 4c and S8), which is consistent with the proposed biosynthetic role of DHS-28 as a β-hydroxyacyl-CoA dehydrogenase.[6,12] Analysis of the *daf-22(ok693)* excretome revealed the absence of all ascarosides with side chains shorter than 12 carbons, as reported earlier (Figures 4c and S8).[5,6,12] We found that *daf-22(ok693)* contains small amounts of homologous series of (ω−1)- and ω-oxygenated long-chain ascarosides featuring saturated (ascr and oscr) and β-hydroxylated side chains (bhas and bhos). In addition, the *daf-22(ok693)* excretome contains VLCAs (>C_{22}) with side-chain lengths of up to 33 carbons, as reported earlier.[5,20]

2.5. Identification of New Indole Ascarosides. Indole-3-carbonylated ascarosides are much less abundant than the corresponding unfunctionalized ascarosides and have recently been shown to function as highly potent aggregation signals.[8] Our LC-MS/MS screen revealed several new types of indole ascarosides (Figure 3c, Tables S5–S8). Using synthetic samples of icas#3, icas#9, and icas#1,[8] we showed that indole ascarosides exhibit a characteristic fragmentation pattern that includes neutral loss of 143 amu [C_9H_5NO] due to cleavage of the indole-3-carbonyl unit, as well as the ascaroside-diagnostic product ion at m/z 73 (see Figure S1). LC-MS/MS screening for components with this fragmentation pattern revealed that known (ω−1)-oxygenated isomers icas#1, icas#9, and icas#10 in *acox-1(ok2257)* are accompanied by a series of ω-oxygenated indole ascarosides (SMIDs icos#1, icos#9, and icos#10), which was confirmed by chemical synthesis of icos#10 as a representative example (see Supporting Information). Peroxisomal β-oxidation mutants that do not produce short-chain ascarosides (<9 carbon side chains), for example, *maoc-1* and *dhs-28* worms, also do not produce any of the corresponding indole ascarosides. Instead, we found that the *maoc-1* and *dhs-28* excretomes contain significant amounts of (ω−1)- and ω-oxygenated long-chain indole ascarosides (SMIDs icas and icos) and indole β-hydroxyascarosides (SMIDs ibha and ibho) with side chains from 9–17 carbons (see Tables S5–S8).

2.6. Indole Ascaroside Biogenesis. Using application experiments with deuterium-labeled tryptophan and axenic *in vitro* cultures, we have previously shown that the indole-3-carbonyl moiety of indole ascarosides originates from L-tryptophan.[8] A similar L-tyrosine or L-phenylalanine origin seems likely for the 4-hydroxybenzoyl moiety of hbas#3, whereas the tigloyl group of mbas#3 could be derived from L-isoleucine.[21] However, it remained unclear at what stage in

ascaroside biosynthesis the indole-3-carbonyl moiety is attached. Comparison of ascaroside and indole ascaroside profiles revealed that indole ascaroside biosynthesis is tightly controlled. For example, we found that in *acox-1* mutants the ω-ascaroside oscr#9 is over 100 times more abundant than the (ω−1)-ascaroside ascr#9, whereas (ω−1)-indole ascaroside icas#9 is much more prominent than ω-indole ascaroside icos#9 (Figure 5a). Similarly, icas#3 and icas#9, the dominating
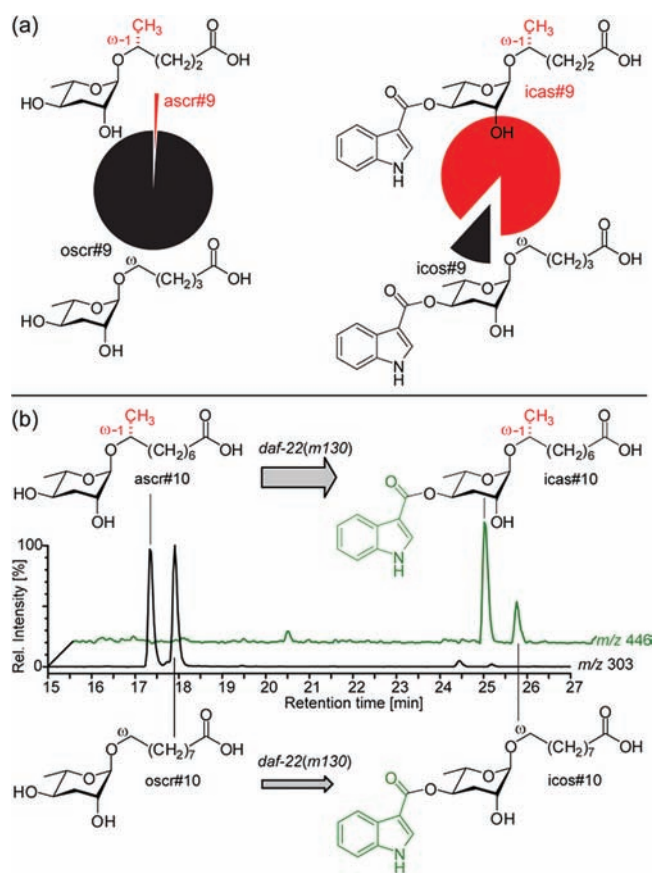

Figure 5. Indole ascaroside biosynthesis. (a) Relative abundance of (ω−1) and ω-oxygenated C_5-ascarosides ascr#9 and oscr#9 and their corresponding indole ascarosides icas#9 and icos#9 in *acox-1* indicates that indole-3-carbonyl attachment is highly specific. (b) LC-MS ion traces of *daf-22(m130)* excretome following incubation with a 1:1 mixture of ascr#10 and oscr#10, showing a preference for indole-3-carbonyl attachment to the (ω−1)-oxygenated ascr#10.

indole ascarosides in the wild-type excretome, are produced in roughly equal amounts, whereas ascr#3 is about 20 times more abundant than ascr#9 (Figure S10). This strong dependence of indole ascaroside biosynthesis on side-chain length and (ω−1)- vs ω-oxygenation suggested that these compounds originate from specific attachment of an indole-3-carbonyl unit to the corresponding non-indole ascarosides.

To test whether non-indole ascarosides serve as precursors for indole ascarosides, we incubated *daf-22(m130)* worms (which are devoid of all short-chain indole and non-indole ascarosides) with a 1:1 mixture of ascr#10 and oscr#10 for 5 days. Subsequent analysis by LC-MS showed partial conversion into icas#10 and icos#10 (Figure 5b), indicating that non-indole ascarosides serve as specific precursors to their corresponding indole derivatives. Moreover, conversion of (ω−1)-ascaroside ascr#10 was preferred over conversion of ω-

ascaroside oscr#10, reflecting the ratios of these compounds in wild-type and *acox-1* mutants. Similarly, we found that *daf-22(m130)* worms convert added ascr#3 into icas#3. Further conversion of indole or non-indole ascarosides into shorter chain derivatives (e.g., ascr#1 or icas#1) was not observed. These results indicate that attachment of an L-tryptophan-derived indole-3-carbonyl unit represents the final step in indole ascaroside biosynthesis.

2.7. Ascaroside Excretion Is Selective. Despite detailed investigations of ascaroside function, little is known about how ascarosides are released and transported from their site of biosynthesis. We compared the ascaroside profiles of the wild-type excretomes (liquid culture supernatant extracts) and worm body metabolomes (worm pellet extracts) to identify possible nonexcreted ascaroside derivatives and to determine quantitative differences. We found that ascaroside profiles of worm pellet extracts differ significantly from those excreted into the media, indicating that ascarosides are differentially released by *C. elegans* (Figure 6a). In the worm pellets, the most abundant
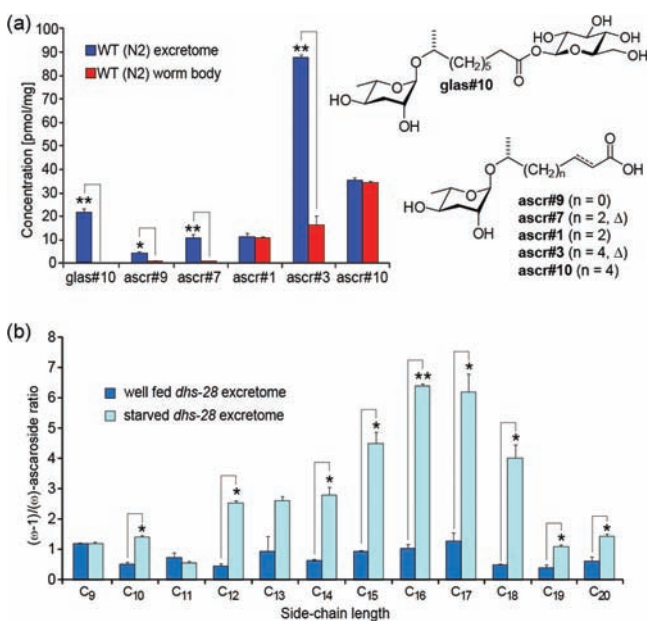

Figure 6. (a) Analysis of worm body ascaroside profiles reveals ascaroside glucosides (e.g., glas#10) and indicates preferential excretion of unsaturated ascarosides. (b) Ratio of $(\omega-1)$- to ω-linked saturated ascarosides in *dhs-28* mutant excretome shows strong dependence on nutritional conditions (for β-hydroxyascarosides see Figure S14), reflecting starvation dependence of ascr#3/ascr#5 ratio in wild-type *C. elegans* (see Figure S15) (Welch's *t* test; * indicates $P < 0.05$; ** indicates $P < 0.001$).

ascarosides, for example ascr#3 in wild-type and ascr#10 in *acox-1* worms, are accompanied by significantly more-polar derivatives, which are absent from the media extracts (Figure S11). MS/MS analysis suggested that these components represent ascaroside *O*-glycoside esters. Isolation of the putative ascr#10 glycoside from *acox-1(ok2257)* worm pellet extracts and subsequent NMR spectroscopic analysis (Figure S12) indicated esterification of ascr#10 with the anomeric hydroxy group of β-glucose, which was subsequently confirmed via synthesis (SMID for 1-β-D-glucosyl ascr#10 is glas#10, Figure 6a). The fact that large quantities of highly polar glas#10 and other ascaroside glucosides (see Table S9) are retained in the worm bodies but not excreted suggests that they represent

transport or storage forms of the ultimately excreted signaling molecules.

In addition, we found that saturated ascarosides are retained in the worm bodies to a much greater extent than their α,β-unsaturated derivatives (Figure 6a). Differential release was also observed for ω-oxygenated components (Figure S13). Therefore, it appears that *C. elegans* exhibits remarkable control over the release of ascaroside signals.

2.8. Nutritional State Affects Ascaroside Biosynthesis. Ascaroside biosynthesis has been reported to depend on various environmental factors including food availability,[6] developmental stage,[15] and temperature.[11] We used LC-MS to investigate the effect of nutritional state on ascaroside biosynthesis by comparing the excretomes of well-fed and starved cultures of wild-type and mutant worms. We found that the ratio of $(\omega-1)$- to ω-linked ascarosides strongly depends on nutritional state. Production of long-chain $(\omega-1)$-oxygenated ascarosides in starved cultures of *dhs-28* was about 5 times higher than those of well-fed cultures (Figures 6b and S14). Similarly, starved wild-type worms excrete significantly larger amounts of the $(\omega-1)$-linked ascr#3 than well-fed worms, relative to the amounts of ω-linked ascr#5 (Figure S15). Both ascr#5 and ascr#3 are major components of the dauer pheromone; however, they affect worm behavior differently.[1,3,4,22]

Therefore, it appears that ascaroside signaling is actively regulated in response to changes in nutrient availability via modulation of $(\omega-1)$ and ω-functionalization of very long-chain fatty acids (VLCFAs) upstream of peroxisomal β-oxidation. Together with the recent finding that ω- and $(\omega-1)$-functionalized ascarosides are sensed by different families of G-protein-coupled receptors,[23] these results suggest that ω- and $(\omega-1)$-functionalized ascarosides target separate downstream signaling pathways.

3. DISCUSSION

Ascarosides play important roles for several different aspects of *C. elegans* biology. This functional diversity is paralleled by corresponding structural diversity and a complex biosynthetic pathway. Our MS/MS-based study revealed 146 ascarosides, including 124 previously unreported analogues, which show several unexpected features including ω-oxygenation of the fatty-acid-derived side chains, 4-hydroxybenzoylation or (*E*)-2-methyl-2-butenoylation of the ascarylose unit, and glucosyl esters. Most ascarosides occur as members of homologous series of compounds with $(\omega-1)$- or ω-linked saturated, α,β-unsaturated, or β-hydroxylated side chains ranging from 3 to 21 (occasionally more) carbons. Importantly, only a few members of each series are produced abundantly in wild-type, and incorporation of specific structural features such as modification in position 4 of the ascarylose (e.g., as in indole ascarosides) or incorporation of α,β-unsaturation appears to be tightly controlled. Given their assembly from carbohydrate, lipid, and amino-acid-derived building blocks, the ascarosides appear as a modular library of small-molecule signals that integrate inputs from three basic metabolic pathways (Figure 7a). The ascarosides then transduce input from these pathways via their diverse signaling functions in *C. elegans*'s behavior and development, including dauer formation, mate attraction, hermaphrodite repulsion, and aggregation.[8,14] Their specific biosyntheses suggest that many of the newly identified ascarosides also contribute to known or as yet undetermined functions in *C. elegans*. As an example, we show that hbas#3 acts

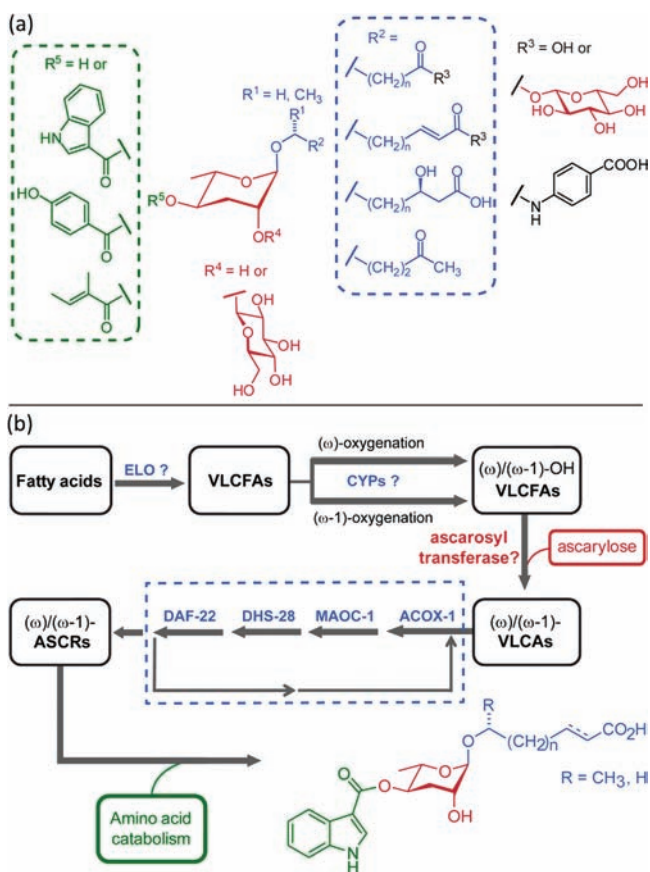**Figure 7.** (a) Modular assembly of ascarosides from amino acid (green), fatty acid (blue), and carbohydrate (red) building blocks. (b) Model for ascaroside biogenesis. Chain elongation of fatty acids (by putative elongase homologues elo-1−9[25]) is followed by (ω−1)- or ω-oxygenation of VLCFAs and ascarylose attachment. The resulting VLCAs enter peroxisomal β-oxidation via ACOX-1, MAOC-1, DHS-28, and DAF-22, producing short-chain ascarosides, which are linked to amino-acid-derived moieties and other building blocks.

as an attraction signal whose potency exceeds that of all previously known small molecules in this model organism. More comprehensive biological evaluation will require consideration of synergistic activities (i.e., testing of compound mixtures), which, given the very large number of compounds, may necessitate high-throughput approaches, for example based on microfluidic devices.[24]

Our results allow us to propose a working model for ascaroside biogenesis (Figure 7b). The finding that ascarosides are members of several homologous series with side chains up to 21 (and more) carbons suggests their origin from peroxisomal β-oxidation of very long-chain precursors. Previous studies reported the presence of VLCAs with C_{29} and C_{31} side chains in wild-type and daf-22 mutants, which could represent precursors or intermediates in ascaroside biosynthesis.[5,20] Alternatively, VLCFAs could undergo peroxisomal β-oxidation prior to (ω−1)- or ω-functionalization and subsequent attachment of the ascarylose. Our observation that the acox-1 mutation affects (ω−1)- and ω-oxygenated ascarosides differently suggests that (ω−1)- and ω-functionalization of VLCFA precursors occurs upstream of their breakdown by peroxisomal β-oxidation. Given the large range in side-chain lengths, it seems likely that resulting (ω−1)- and ω-hydroxy VLCFAs are linked to ascarylose prior to entering the β-oxidation pathway,

though the presence of a promiscuous ascarosyl transferase cannot be excluded (Figure 7b).

Chain shortening of VLCA then progresses via repetitive cycles of peroxisomal β-oxidation. The results from our LC-MS/MS screen allow us to propose precise roles for enzymes participating in each of the four steps of the β-oxidation cycle: acyl-CoA oxidase ACOX-1, enoyl-CoA hydratase MAOC-1, β-hydroxyacyl-CoA dehydrogenase DHS-28, and β-ketoacyl-CoA thiolase DAF-22. We show that mutations in acox-1, maoc-1, and dhs-28 result in specific changes of the corresponding ascaroside profiles, in agreement with their proposed functions.

The acyl-CoA oxidase ACOX-1 has been the subject of a previous study which suggested that mutations in acox-1 primarily affect the biosynthesis of ascr#2 and ascr#3, but not of ascr#1.[11] However, our results indicate that acox-1(ok2257) mutants have a reduced ability to process C_9 (ω−1)-functionalized ascarosides, resulting in diminished production of all shorter-chained ascarosides and buildup of C_9 and longer-chained saturated ascarosides. Mutations of maoc-1 (as well as dhs-28 and daf-22) have been shown to result in expansion of intestinal lipid droplets and cause an increase in fasting- and lipolysis-resistant triglycerides.[19] Our results show that MAOC-1 participates in ascaroside biosynthesis, acting as the previously unidentified enoyl-CoA hydratase. These findings further demonstrate that hydration of enoyl-CoAs and dehydrogenation of β-hydroxyacyl-CoAs in C. elegans are catalyzed by two distinct enzymes, MAOC-1 and DHS-28, as had been suggested on the basis of their homology to separate functional domains of human MFE-2.[19]

We further show that attachment of the tryptophan-derived indole-3-carbonyl unit in indole ascarosides likely represents the last step in their biosynthesis, and that this step is highly specific. As attachment of an indole-3-carbonyl group to ascarosides can dramatically alter their biological function, such tight regulation makes sense. For example, indole-3-carbonyl addition to the dauer-inducing and strongly repulsive signal ascr#3 results in the potent hermaphrodite attractant icas#3.[8] Therefore, identification of the enzymes that attach indole-3-carbonyl and other functional groups to the ascarosides will be of great interest.

The biosynthesis of ascarylose in C. elegans has not been investigated, but detection of ascarosides in axenic C. elegans cultures demonstrated that C. elegans produce ascarylose endogenously.[8] Ascarylose biosynthesis in bacteria is well understood, and the C. elegans genome includes several homologues of bacterial genes in this pathway, for example, ascE from Yersinia pseudotuberculosis (Figure S16),[26] providing potential entry points for the study of ascarylose biosynthesis and its regulation in nematodes. In addition, the oxidases catalyzing (ω−1)- or ω-functionalization of VLCFA precursors remain to be identified. Our finding that the ratio of (ω−1)/ω-oxygenated ascarosides in wild-type and peroxisomal β-oxidation mutants is strongly affected by starvation suggests that this step may encode information about nutritional state. Finally, we demonstrate that ascaroside excretion is surprisingly specific. Given the high sensitivity and selectivity of LC-MS/MS, we believe that ascaroside profiling using this method will aid identification of additional genes and environmental factors that participate in ascaroside biosynthesis and homeostasis.

ASSOCIATED CONTENT

Ⓢ Supporting Information

Detailed experimental procedures including the synthesis of reference compounds, a full list of identified ascarosides, and their LC-MS and NMR spectroscopic data. This material is available free of charge via the Internet at http://pubs.acs.org.

AUTHOR INFORMATION

Corresponding Author

schroeder@cornell.edu

ACKNOWLEDGMENTS

REFERENCES

(1) Jeong, P. Y.; Jung, M.; Yim, Y. H.; Kim, H.; Park, M.; et al. *Nature* **2005**, *433*, 541−545.

(2) Butcher, R. A.; Fujita, M.; Schroeder, F. C.; Clardy, J. *Nat. Chem. Biol.* **2007**, *3*, 420−422.

(3) Srinivasan, J.; Kaplan, F.; Ajredini, R.; Zachariah, C.; Alborn, H. T.; Teal, P. E.; Malik, R. U.; Edison, A. S.; Sternberg, P. W.; Schroeder, F. C. *Nature* **2008**, *454*, 1115−1118.

(4) Butcher, R. A.; Ragains, J. R.; Kim, E.; Clardy, J. *Proc. Natl. Acad. Sci. U.S.A.* **2008**, *105*, 14288−14292.

(5) Pungaliya, C.; Srinivasan, J.; Fox, B. W.; Malik, R. U.; Ludewig, A. H.; Sternberg, P.; Schroeder, F. C. *Proc. Natl. Acad. Sci. U.S.A.* **2009**, *106*, 7708−7713.

(6) Butcher, R. A.; Ragains, J. R.; Li, W.; Ruvkun, G.; Clardy, J.; Mak, H. Y. *Proc. Natl. Acad. Sci. U.S.A.* **2009**, *106*, 1875−1879.

(7) (a) Ren, P.; Lim, C. S.; Johnsen, R.; Albert, P. S.; Pilgrim, D.; Riddle, D. L. *Science* **1996**, *274*, 1389−1391. (b) Kimura, K. D.; Tissenbaum, H. A.; Liu, Y.; Ruvkun, G. *Science* **1997**, *277*, 942−946. (c) Schroeder, F. C. *ACS Chem. Biol.* **2006**, *1*, 198−200. (d) Fielenbach, N.; Antebi, A. *Genes Dev.* **2008**, *22*, 2149−2165. (e) Sommer, R. J.; Ogawa, A. *Curr. Biol.* **2011**, *21*, R758−R766.

(8) Srinivasan, J.; von Reuss, S. H.; Bose, N.; Zaslaver, A.; Mahanti, P.; Ho, M.; O'Doherty, O.; Edison, A.; Sternberg, P.; Schroeder, F. C. *PLoS Biol.* **2012**, *10*, e1001237.

(9) Golden, J. W.; Riddle, D. L. *Mol. Gen. Genet.* **1985**, *198*, 534−536.

(10) White, J. Q.; Nicholas, T. J.; Gritton, J.; Truong, L.; Davidson, E. R.; Jorgensen, E. M. *Curr. Biol.* **2007**, *17*, 1847−1857.

(11) Joo, H. J.; Kim, K. Y.; Yim, Y. H.; Jin, Y. X.; Kim, H.; Kim, M. Y.; Paik, Y. K. *J. Biol. Chem.* **2010**, *285*, 29319−29325.

(12) Joo, H. J.; Yim, Y. H.; Jeong, P. Y.; Jin, Y. X.; Lee, J. E.; Kim, H.; Jeong, S. K.; Chitwood, D. J.; Paik, Y. K. *Biochem. J.* **2009**, *422*, 61−71.

(13) Butcher, R. A.; Ragains, J. R.; Clardy, J. *Org. Lett.* **2009**, *11*, 3100−3103.

(14) Edison, A. S. *Curr. Opin. Neurobiol.* **2009**, *19*, 378−388.

(15) Kaplan, F.; Srinivasan, J.; Mahanti, P.; Ajredini, R.; Durak, O.; Nimalendran, R.; Sternberg, P. W.; Teal, P. E. A.; Schroeder, F. C.; Edison, A. E.; Alborn, H. T. *PLoS ONE* **2011**, *6*, e17804.

(16) "SMID" indicates s̲mall m̲olecule id̲entifier for small molecules identified from *C. elegans* and other nematodes. The SMID database (www.smid-db.org) is an electronic resource maintained by Frank C. Schroeder and Lukas Mueller at the Boyce Thompson Institute in collaboration with Wormbase (www.wormbase.org). The purpose of this database is to introduce searchable, gene-style identifiers— "SMIDs"—for all small molecules newly identified from *C. elegans* and other nematodes.

(17) (a) Rittschof, D.; Cohen, J. H. *Peptides* **2004**, *25*, 1503−1516. (b) Gozes, I.; Morimoto, B. H.; Tiong, J.; Fox, A.; Sutherland, K.; Dangoor, D.; Holser-Cochav, M.; Vered, K.; Newton, P.; Aisen, P. S.; Matsuoka, Y.; van Dyck, C. H.; Thal, L. *CNS Drug Rev.* **2005**, *11*, 353−368.

(18) Haataja, T. J. K.; Koski, M. K.; Hiltunen, J. K.; Glumoff, T. *Biochem. J.* **2011**, *435*, 771−781.

(19) Zhang, S. O.; Box, A. C.; Xu, N.; Le Men, J.; Yu, J.; Guo, F.; Trimble, R.; Mak, H. Y. *Proc. Natl. Acad. Sci. U.S.A.* **2010**, *10*, 4640−4645.

(20) Zagoriy, V.; Matyash, V.; Kurzchalia, T. *Chem. Biodivers.* **2010**, *7*, 2016−2022.

(21) Attygalle, A. B.; Wu, X.; Will, K. W. *J. Chem. Ecol.* **2007**, *33*, 963−970.

(22) Macosko, E. Z.; Pokala, N; Feinberg, E. H.; Chalasani, S. H.; Butcher, R. A.; Clardy, J.; Bargmann, C. I. *Nature* **2009**, *458*, 1171−1175.

(23) (a) Kim, K.; Sato, K.; Shibuya, M.; Zeiger, D. M.; Butcher, R. A.; Ragains, J. R.; Clardy, J.; Touhara, K.; Sengupta, P. *Science* **2009**, *326*, 994−998. (b) McGrath, P. T.; Xu, Y.; Ailion, M.; Garrison, J. L.; Butcher, R. A.; Bargmann, C. I. *Nature* **2011**, *477*, 321−325.

(24) Chung, K.; Zhan, M.; Srinivasan, J.; Sternberg, P. W.; Gong, E.; Schroeder, F. C.; Lu, H. *Lab Chip* **2011**, *11*, 3689−3697.

(25) Agbaga, M. P.; Brush, R. S.; Mandal, N. A.; Henry, K.; Elliott, M. H.; Anderson, R. E. *Proc. Natl. Acad. Sci. U.S.A.* **2008**, *105*, 12843−12848.

(26) Thorson, J. S.; Lo, S. F.; Olivier, P.; He, X.; Liu, H. W. *J. Bacteriol.* **1994**, *176*, 5483−5493.